

Reevaluation of Photoluminescence Intensity as an Indicator of Efficiency in Perovskite Solar Cells

Valerio Campanari, Faustino Martelli,* Antonio Agresti, Sara Pescetelli, Narges Yaghoobi Nia, Francesco Di Giacomo, Daniele Catone, Patrick O'Keeffe, Stefano Turchini, Bowen Yang, Jiajia Suo, Anders Hagfeldt, and Aldo Di Carlo*

The photoluminescence (PL) intensity is often used as an indicator of the performance of perovskite solar cells and indeed the PL technique is often used for the characterization of these devices and their constituent materials. Herein, a systematic approach is presented to the comparison of the conversion efficiency and the PL intensity of a cell in both open-circuit (OC) and short-circuit (SC) conditions and its application to multiple heterogeneous devices. It is shown that the quenching of the PL observed in SC conditions is a good parameter to assess the device efficiency. The authors explain the dependence of the PL quenching ratio between OC and SC on the cell efficiency with a simple model that is also able to estimate the carrier extraction time of a device.

1. Introduction

As for most semiconductors, steady-state photoluminescence (PL) (or continuous-wave PL, cw-PL) is extensively used to characterize perovskite solar cells (PSCs). The PL intensity and spectrum are not only used to investigate the properties of the constituent materials but are also often directly linked to the device efficiency. The carrier density in semiconductors under illumination is determined by the recombination dynamics of charge carriers that can be summarized by the simplified rate equation^[1–3]

$$\frac{dn}{dt} = -k_1^{\text{oc}}n - k_2n^2 - k_3n^3 + g = 0 \quad (1)$$

where n is the electronic charge carrier density, k_1^{oc} is the first-order Shockley–Read–Hall (SRH) recombination (nonradiative) rate constant, k_2 is the second-order band-to-band (radiative) recombination rate constant, k_3 is the third-order Auger (nonradiative) recombination rate constant, and g is the generation rate. We specified a particular value of k_1 for open-circuit (OC) conditions (k_1^{oc}) to distinguish it in general from the SRH rate at short-circuit (SC) (that we will indicate as k_1^{sc}). Ideally, for a perfectly homogeneous device, they should be equal but any kind of device inhomogeneity in terms of recombination centers (e.g., at interfaces respect to the bulk), together with the change of carrier distribution occurring between OC and SC conditions, can create a discrepancy between these two values. The need for this correction will be explained more clearly in the discussion of results and in the Supporting Information (SI).

Under steady-state conditions, such as those of a cw-PL measurement, the variation of carrier density over time is zero. Once a certain density of excited carriers is produced by illumination, the amount of radiative recombination will be determined by the competition between the radiative ($\propto k_2n^2$) and the nonradiative recombination ($\propto k_1^{\text{oc}}n$). In general, at the carrier density typically photoexcited in operating solar cells, we can neglect the Auger recombination and the most important limitation to PL emission is the SRH recombination. When a perovskite film is placed between two transport materials and metal contacts, forming a solar cell, the dynamics of the charge carriers is modified with respect to the bare perovskite layer. The presence of selective materials for the extraction of electrons and holes makes it

V. Campanari, A. Agresti, S. Pescetelli, N. Y. Nia, F. Di Giacomo, A. Di Carlo

CHOSE (Centre for Hybrid and Organic Solar Energy)

Department of Electronic Engineering

University of Rome Tor Vergata

Via del Politecnico 1, 00133 Rome, Italy

E-mail: aldo.dicarlo@ism.cnr.it

F. Martelli

CNR-IMM

Area della Ricerca di Roma Tor Vergata

100 Via del Fosso del Cavaliere, 00133 Rome, Italy

E-mail: faustino.martelli@cnr.it

D. Catone, S. Turchini, A. Di Carlo

Istituto di Struttura della Materia – CNR (ISM-CNR)

EuroFEL Support Laboratory (EFSL)

Area della Ricerca di Roma Tor Vergata

Via del Fosso del Cavaliere 100, 00133 Rome, Italy

P. O'Keeffe

Istituto di Struttura della Materia – CNR (ISM-CNR)

EuroFEL Support Laboratory (EFSL)


Area della Ricerca di Roma 1, 00015 Monterotondo Scalo, Italy

B. Yang, J. Suo, A. Hagfeldt

Department of Chemistry - Ångström Laboratory

Uppsala University

Box 523, SE-75120 Uppsala, Sweden

 The ORCID identification number(s) for the author(s) of this article can be found under <https://doi.org/10.1002/solr.202200049>.

© 2022 The Authors. Solar RRL published by Wiley-VCH GmbH. This is an open access article under the terms of the Creative Commons Attribution License, which permits use, distribution and reproduction in any medium, provided the original work is properly cited.

DOI: 10.1002/solr.202200049

possible to separate the excited carriers and generate power from the device when it is placed in an external circuit. Under solar cell operation, both nonradiative recombination and extraction of charge carriers from the active layers contribute to the reduction of the PL intensity, subtracting carriers from the radiative recombination process, while having an opposite impact on device performances: nonradiative recombination is detrimental for device efficiency while an extraction faster than any carrier recombination is desirable. Indeed, we can consider the extraction of the carriers from the cell as a phenomenon which competes with the other channels of recombination

$$\frac{dn}{dt} = -k_1^{sc}n - \frac{I_{sc}}{qV} - k_2n^2 + g = 0 \quad (2)$$

where I_{sc} is the SC current, V the device volume, and q the elementary charge.

To provide a detailed model of carrier dynamics in these conditions, we would require a numerical solution of the drift diffusion equations. However, in the framework of this work, as it will be clarified later, we can approximate I_{sc} simply by introducing a second linear nonradiative term, namely, the extraction rate ($k_e = 1/\tau_e$), that underlies all the processes involved in carrier separation and extraction (more details in SI). The rate Equation (2) then becomes

$$\frac{dn}{dt} = -(k_1^{sc} + k_e)n - k_2n^2 + g = 0 \quad (3)$$

As already mentioned, to be general we considered a different value of k_1 for SC.

cw-PL is often able to provide important information about materials and device physics. For example, the PL quantum yield (PLQY) of a perovskite film can be directly linked to the quasi-Fermi-level splitting (QFLS), establishing the ideal V_{oc} of a photovoltaic device. This information can be used to evaluate different features of a PSC, like bulk recombination and surface recombination.^[4,5]

In a complete device, an often used equation, based on the reciprocity relation, links PLQY to V_{oc} .^[6–8]

$$V_{oc} = V_{oc}^{rad} - \frac{k_B T}{q} |ln(\eta)| \quad (4)$$

where V_{oc}^{rad} is the maximum theoretical V_{oc} achievable at the radiative limit, η is the PL (or electroluminescence, EL) quantum yield, k_B is the Boltzmann constant, and q is the elementary charge. This equation indicates that the V_{oc} loss of the solar cell with respect to its radiative limit is mostly determined by the nonradiative recombination due to defects. However, the use of Equation (4), that represents a general model in the field of photovoltaic devices, suffers from simplifications that are critical to delicate materials like perovskites and to the devices in which they are used.^[4,9,10]

In general, all the information that can be extracted from the PL should be always analyzed taking into account the variables that arise from the strong nonideality and great variability of perovskite materials and the related devices.

The intensity of cw-PL is also used to directly compare PSCs performances while neglecting some important features. An

example of characterization method that is sometimes used to establish the quality of PSCs is to consider the PL quenching occurring when a bare perovskite layer is embedded in a more complex structure containing one or more transport layers. The claim is that a greater quenching induced by the cell structure embedding the perovskite layer corresponds to a better carrier separation^[11–17] and hence to a potentially greater cell efficiency. However, those measurements are always performed in OC conditions (in most of the cases the device is simply disconnected), where no charge carrier is truly extracted from the device. Under these conditions, we can only imagine a partial polarization of the charge carrier distribution, due to their accumulation near the respective interfaces to compensate the build-in electric field generated by the band alignment of all the materials forming the solar cell. The reduction of the PL intensity for a device with respect to a bare film is instead induced by the enhancement of nonradiative loss because of the creation of nonradiative defective centers at the interfaces^[18,19] and cannot be uniquely considered a sign of better carrier extraction for a particular cell structure. In general, the overall evaluation of the device performances cannot be provided by single PL measurements at OC because they do not take into account the carrier extraction in the working cell.

An approach, that overcomes some of the previous limitations, is to consider the PL intensity in different device operating conditions. In this way the carrier extraction capacity of the solar cell can also be considered. Many studies have investigated the behavior of PL intensity at different bias voltage conditions, both in PSCs^[19–22] and in solar cells based on other technologies.^[23–25] For example, it has been found that the PL intensity, taken at a range of solar cell voltages, accurately reflects the J - V curve of the same device, giving also the opportunity to obtain information on the fill factor (FF)^[19] directly from the variation of PL when the operating cell is driven from OC to the maximum power point (MPP) conditions.

Further, simple analyses to include the real device characteristics were performed comparing the PL quenching between OC and SC conditions.^[21,26–28] In particular, Du et al.^[21] found a linear relationship between the logarithm of the PL quenching and the power conversion efficiency (PCE) or the V_{oc} . This linear relationship was found by analyzing three devices containing the same absorbing layer.

Owing to the simplicity and fast use of the proposed approach that does not make use of a biasing supply (only OC and SC conditions are required), we define the model and the procedure to properly compare the performances of different PSCs in a very general way. To understand the versatility of this characterization technique, it is important to compare systematically a large number of heterogeneous devices with different architectures and coming from different runs. Moreover, there is another, well-known but often neglected, aspect that should be considered to design a reliable characterization technique based on PL that can be of broad use: the PL intensity in perovskites is not stable over time and can undergo both increasing and decreasing trends that can occur both on short (seconds and minutes) or long timescales (hours).^[29–38] This peculiar behavior can have significant impact on the characterization results.

In this work, we measure the cw-PL at 1 sun, in both OC and SC conditions, of several perovskite-based solar cells with

different active layers, charge transporting layers, and device structures. These cells have different performances with their PCE ranging from 5.63% to 21.5%. We show that the straightforward technique based on the quenching ratio between PL_{oc} and PL_{sc} (PL under SC conditions) can be directly used to evaluate the PSC performances with a surprisingly high level of generality and precision despite all the involved approximations, simultaneously giving information on the characteristic time for carrier extraction in the photovoltaic devices. We also show that the dependence of the PL intensity on the illumination time, which is generally neglected, must be taken into account in any attempt to provide a reliable characterization of PSCs based on PL.

2. Devices and Design of the Experiment.

The main aim of our experiment is to test in a systematic way the relationship between the performances of PSCs and the cw-PL under different operating conditions. Our intention is twofold: verify if a reliable and established figure of merit (FOM) exists, which can be defined with a simple PL experiment (refining the experimental protocol to make it as precise as possible) and also to obtain from it further information on carrier dynamics in the device. The experiments were therefore performed on a large number of different device structures.

Starting from the works of Stolterfoht et al.^[19] and Du et al.,^[21] we will propose a FOM based on a simple formula that uses the relative intensity quenching (PLQ_{oc-sc}) between PL_{oc} and PL_{sc} (i.e., PL at SC)

$$PLQ_{oc-sc} = \frac{PL_{oc} - PL_{sc}}{PL_{oc}} \quad (5)$$

Referring to Equations (1) and (3) we can associate a simplified meaning to this value. Solving Equations (1) and (3) in steady-state conditions (see SI for details about the model), where $dn/dt = 0$, we can find the carrier concentration in both OC ($n_{oc}(k_1^{oc})$) and SC conditions ($n_{sc}(k_1^{sc}, k_e)$). Using these values we can estimate the rate of emitted photons, that is proportional to the PL ($\propto k_2 n^2$), and consequently

$$PLQ_{oc-sc} = \frac{(n_{oc}(k_1^{oc}))^2 - (n_{sc}(k_1^{sc}, k_e))^2}{(n_{oc}(k_1^{oc}))^2} \quad (6)$$

We can also extrapolate from the model the approximate relationship, $PCE = (V_{oc} I_{sc} FF) / P_{in}$, where V_{oc} is the open-circuit voltage, I_{sc} is the short-circuit current, FF is the fill factor, and P_{in} is the input light power. Indeed, we can approximate I_{sc} from the value of k_e as $I_{sc} = qV k_e n_{sc}$ where V is the perovskite volume and V_{oc} as $qV_{oc} \approx QFLS = k_B T \ln(n_{oc}(k_1^{oc})^2 / n_i^2)$ ^[4] where n_i is the intrinsic carrier concentration. The value of the FF is not evaluable by the model and is considered to be constant.

If we plot PLQ_{oc-sc} versus PCE while varying randomly k_1^{oc} and k_e (see Figure S1a and Figure S1b in SI), it is possible to observe that the resulting curve is mainly dependent on the ratio between k_e and k_1^{oc} and only slightly on their absolute values. It is also possible to observe that the higher the extraction rate with respect to the nonradiative recombination rate, the greater is the value of PLQ_{oc-sc} and PCE. Moreover, the relation between the log of PLQ_{oc-sc} and PCE is not linear

and the curve describing the relationship between the two follows a saturating trend.

Our aim is to test the validity of this relation by measuring the PL_{oc} and the PL_{sc} of a heterogeneous set of devices, designed to provide different performances (Table 1). In particular, we decided to vary not only the single transport layers, as often made in such comparisons, but also the perovskite itself and the whole cell structure, aspects that are usually not varied in this kind of comparison. In three PSCs a single cation $MAPbI_3$ (M) perovskite was used as the active material, while in all the other cells the active layer was a triple cation, mixed halide (T) perovskite $((Cs_{y1}MA_{y2}FA_{y3})Pb(I_{1-x}Br_x)_3)$. All the devices are summarized in Table 1. To underline the importance of taking into account materials and/or device variability, we highlight that T devices are produced in different runs, indicated by a number (T1, T2, T3, T4, and T5) and that in some cases the triple cation perovskite was also prepared with different processes and with slightly different resulting stoichiometry indicated by a letter A, B, C in Table 1 (the details of production are reported in SI). In all the devices, except for T4 and T5, a TiO_2 electron transport layer (ETL) was used. In the two M solar cell types, the hole transport layer (HTL) was different, in particular we used Spiro-MeOTAD and a copper derivative corrole Cu^tBuTPC .^[39] Both the T1-based devices have Spiro-MeOTAD as the HTL, but in one of them we added an interlayer based on phenethylammonium iodide (PEAI) that is used for surface passivation and to favor the charge carrier transfer into the HTL^[40]. The T2 and T3 devices have two different HTLs ((poly[bis(4-phenyl)(2,5,6-trimethylphenyl)amine] hereafter (PTAA) and poly(3-hexylthiophene) hereafter (P3HT) and for both structure different MW of polymers were applied and investigated.^[41,42] T4 and T5 devices^[43] have an inverted structure (see Table 1) with NiOx as the HTL and two different ETLs. Finally, also the T6 devices have Spiro-MeOTAD and TiO_2 as the HTL and the ETL, respectively, but with a different passivation based on 2-cyclohexylethylammonium iodide (CEAI).

A FOM such as PLQ_{oc-sc} cannot discriminate among devices with different absorption coefficients. For example, if an active material has a bandgap that is much larger than another one, but a similar PLQ_{oc-sc} , the PCE of the first material will be overestimated. In the analysis of our results the differences in the absorption are expected to be very small but, in any case, we have taken into account this small difference in the bandgaps for M, T4, T5, and T6^[44-48] and have suitably corrected the values PLQ_{oc-sc} normalizing them with respect to the other devices (more details in SI).

For each device we first measured the characteristic parameters (V_{oc} , J_{sc} , FF, and PCE) through a standard $J-V$ characterization to determine the reference values for the device performances. PSCs can suffer from low reproducibility and even with the same manufacturing process sometimes different device efficiencies are achieved. In such cases, we performed the PL measurements also on two nominally equal devices if they showed significantly different performances.

All devices were masked with a 0.1 cm^2 mask to normalize the device area that was illuminated with a white light from a LED illuminator at 1 sun. We chose to excite the device with a continuous white spectrum instead of a monochromatic (and/or pulsed) light, as is often used for PL characterization,

Table 1. Summary of the analyzed devices and related reference performances M, T1, T2, T3, T4 T5, and T6 in the device name indicate the specific production runs, while the letters a, B, C differences in material preparation. for details, see Supporting Information.

PCE [%]	FF	J_{sc} [mA cm^{-2}]	V_{oc} [V]	Device name	Device structure
17.8	80.07	20.41	1.089	M-Spiro[1]	c-TiO ₂ /m-TiO ₂ /MAPbI ₃ /Spiro-OMeTAD
17.17	81.65	19.56	1.075	M-Spiro[2]	c-TiO ₂ /m-TiO ₂ /MAPbI ₃ /Spiro-OMeTAD
8.77	72.11	12.89	0.944	M-Corrole	c-TiO ₂ /m-TiO ₂ /MAPbI ₃ /Cu-corrole
15.1	69.72	21.07	1.028	T1-Spiro	c-TiO ₂ /m-TiO ₂ /Triple Cation(A)/Spiro-MeOTAD
16.71	72.96	21.43	1.069	T1-P-Spiro [1]	c-TiO ₂ /m-TiO ₂ /Triple Cation(A)/PEAI/Spiro-MeOTAD
16.34	73.14	20.95	1.067	T1-P-Spiro [2]	c-TiO ₂ /m-TiO ₂ /Triple Cation(A)/PEAI/Spiro-MeOTAD
17.71	76.67	22.49	1.027	T2-PTAA(115)[1]	c-TiO ₂ /m-TiO ₂ /Triple Cation(B)/PTAA(115 kDa)
18.78	78.95	23.19	1.026	T2-PTAA(115)[2]	c-TiO ₂ /m-TiO ₂ /Triple Cation(B)/PTAA(115 kDa)
17.06	73.56	22.3	1.04	T2-P3HT(85)	c-TiO ₂ /m-TiO ₂ /Triple Cation(B)/P3HT(85 kDa)
13.37	67.19	20.33	0.979	T3-PTAA(10)	c-TiO ₂ /m-TiO ₂ /Triple Cation(B)/PTAA(10 kDa)
12.97	72.15	17.34	1.037	T3-P3HT(20-45)[1]	c-TiO ₂ /m-TiO ₂ /Triple Cation(B)/P3HT(20-45 kDa)
9.25	63.69	14.53	1	T3-P3HT(20-45)[2]	c-TiO ₂ /m-TiO ₂ /Triple Cation(B)/P3HT(20-45 kDa)
15.55	78.06	19.24	1.036	T3-PTAA(390)[2]	c-TiO ₂ /m-TiO ₂ /Triple Cation(B)/PTAA(390 kDa)
5.63	34.9	17.97	0.898	T4-Al ₂ O ₃	NiOx/Triple Cation(C)/p-Al ₂ O ₃ /C60/BCP
13.4	65.7	19.6	1.036	T5-PC1BM[1]	NiOx/Triple Cation(C)/PCBM/BCP
17.5	74.5	19.8	1.067	T5-PCBM[2]	NiOx/Triple Cation(C)/PCBM/BCP
21.5	75.6	25	1.14	T6-P-SPIRO[1]	c-TiO ₂ /m-TiO ₂ /triple Cation(D)/CEAI/Spiro[1]
20.5	75.2	24.1	1.13	T6-P-SPIRO[2]	c-TiO ₂ /m-TiO ₂ /triple Cation(D)/CEAI/Spiro[2]

because the excitation conditions can modify the PL response of the perovskites^[49,50] and because we want to use excitation conditions as similar as possible to the operational ones. Monochromatic excitation for example can also produce a different penetration depth profile of the light in the absorbing layer with respect to the white light, thus leading to a change in the excited carrier density profile. On the other hand, if the light source is pulsed, while at the same time maintaining a mean power density equal to device operation conditions, it would induce a different carrier distribution and dynamics with respect to the continuous case. The temporal change of PL_{oc} and PL_{sc} intensities impacts the evaluation of PLQ_{oc-sc}. The most reliable correlation between PL quenching and conversion efficiency has been found using the values of PL_{oc} and PL_{sc} measured in the first minute of illumination after the first fast transient (see SI for more details). In this time span, we first measure the PL intensity in OC and SC conditions taking the values measured immediately before and after the switch from OC to SC. Then we repeated the measurement to investigate the PL variation both in OC and SC (more details on the procedure and the reasons behind our choices are reported in SI).

In Figure 1a we report a qualitative schematic representation of the experimental procedure and in Figure 1b a representative PL spectrum, extracted from our data, as an example of PL quenching between OC and SC.

3. Results and Discussion

We can observe a distribution of efficiency not only for different types of devices but also, sometimes, for different devices of the

same batch, as reported in Table 1. The devices have efficiencies ranging between $\approx 5\%$ and $\approx 21\%$, which is a sufficiently wide range to provide a significant comparison. In order to verify a statistical correlation between the experimental PLQ_{oc-sc} (computed using Equation (5) corrected for the absorption coefficient) and the device efficiency, we report the former quantity as a function of the latter on a logarithmic scale in Figure 2.

In the figure the symbols representing the devices are divided by color into seven groups determined by their production run (M, T1, T2, T3, T4, T5, and T6) and then distinguished by different shapes within any given group. We observe a clear correlation between the two quantities: log(PLQ_{oc-sc}) and PCE (Figure 2) that can be explained through Equation (1) and (3) (gray region in Figure 2), as reported in the previous section. As it is clear from Figure 2, the saturation of the log(PLQ_{oc-sc}) values means that the sensitivity of the method is lower at very high efficiencies.

In Figure 3a,b we report the same values of PL_{oc} used in Equation (5) versus V_{oc} and PCE, respectively. In Figure 3c we did the same for PL_{sc} versus PCE, a figure that allows for some important considerations. It is not possible to obtain a general correlation among all the devices. PL_{oc} fails to predict device performances if a heterogeneous group of devices is taken into account. We also observe that not even a nominally identical active material guarantees this kind of relation. For the sake of a quick comparison, in Figure 3 we group the devices with different highlighting colors.

These results will be explained in the light of an interpretation based on our model previously presented by using Eqs. (1) and (3) (see also SI). In OC conditions all the carriers must recombine

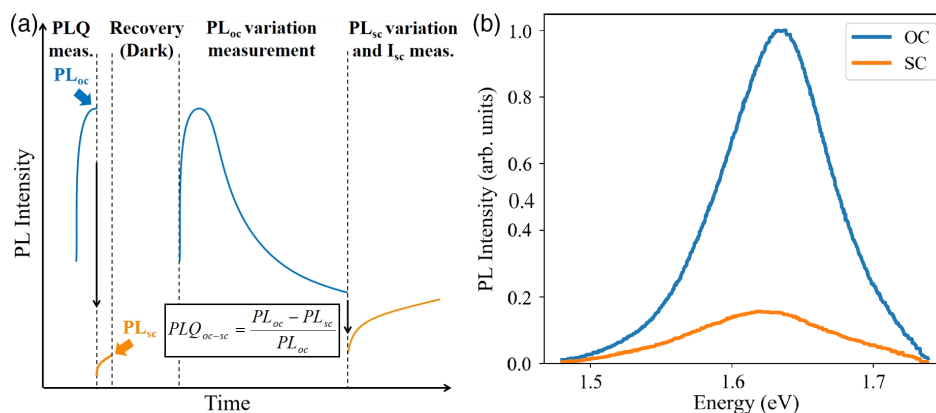


Figure 1. a) Qualitative representation of the experimental procedure that shows the value used as PL_{oc} and PL_{sc} and the following observed PL variations at OC and SC. b) PL spectra at OC and SC selected from our data only for representative purpose.

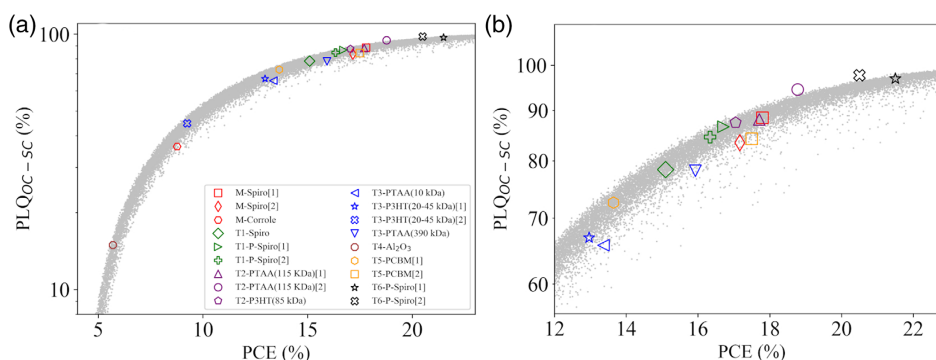


Figure 2. a) Logarithmic plot of the PL quenching (PLQ_{oc-sc}) moving from OC to SC conditions (expressed by Equation (5)) versus PCE. Each color represents a particular production run. The gray set of points is calculated from the model with randomly selected values of k_1^{oc} and k_e (see SI for details). b) A zoom-in of the panel “a” for high efficiencies.

inside the device because they cannot be extracted from it (Equation (1)). Therefore, the PL in OC conditions only reveals the number of carriers that recombine radiatively but does not provide information on the carrier density contributing to the device operation. It was shown that in perovskites nonradiative recombination is the dominant pathway that determines the carrier lifetime ($k_1 \gg n \cdot k_2$).^[1,51,52] A higher rate of nonradiative loss (k_1^{oc}) contributes to the decrease of the PL as well as the device V_{oc} and PCE. On the other hand, the radiative recombination rate (k_2) also plays a role to determine the PL intensity. A higher rate of radiative recombination contributes to the increase of the PL intensity regardless of the value of carrier lifetime imposed by k_1^{oc} although, of course, a competition between the two recombination paths always exists, where the faster one is favored. This consideration can explain the reason for the scattered data shown in Figure 3a,b,c if we suppose that not only k_1^{oc} can change in such an inhomogeneous set of devices, but also k_2 : a variation of k_2 should affect the value of PL_{oc} , while PCE and V_{oc} are only dependent on k_1^{oc} and k_e . It was observed that in perovskites the radiative recombination rate (k_2) can vary.^[53–55] Another parameter that can influence the results in Figure 3 is the slight variability of perovskite thickness among different device production runs, even if small, a

difference in film volumes can produce significantly different PL emission.

The PL intensity in SC conditions (obtainable from Equation (3)), on the other hand, is proportional to the carriers that do not leave the device before their radiative recombination. Combining both PL_{sc} and PL_{oc} through Equation (5), we take into account the carriers that actually contribute to the cell operation compared to the total number of carriers available, providing more accurate information about the link between PL and PCE. The general trend of the curve in Figure 2 can be explained through Equations (1) and (3), as reported in the previous section.

In our model FF is taken to be constant. To evaluate the impact of this approximation, we report in Figure S2a, Supporting Information a plot similar to that of Figure 2, in which the FF is varied in a similar manner to that performed for k_1^{oc} and k_e . The result is that the dispersion of the points on the graph is slightly increased but the trend is well conserved. We point out that the data scattering mainly affects those devices that have a small FF like “T4- Al_2O_3 .” This aspect can be a coincidence and deserves further investigations.

Similarly, in the SI we also report a plot (Figure S2b, Supporting Information) of PLQ_{oc-sc} versus J_{sc}/J_{SQ} , where J_{SQ}

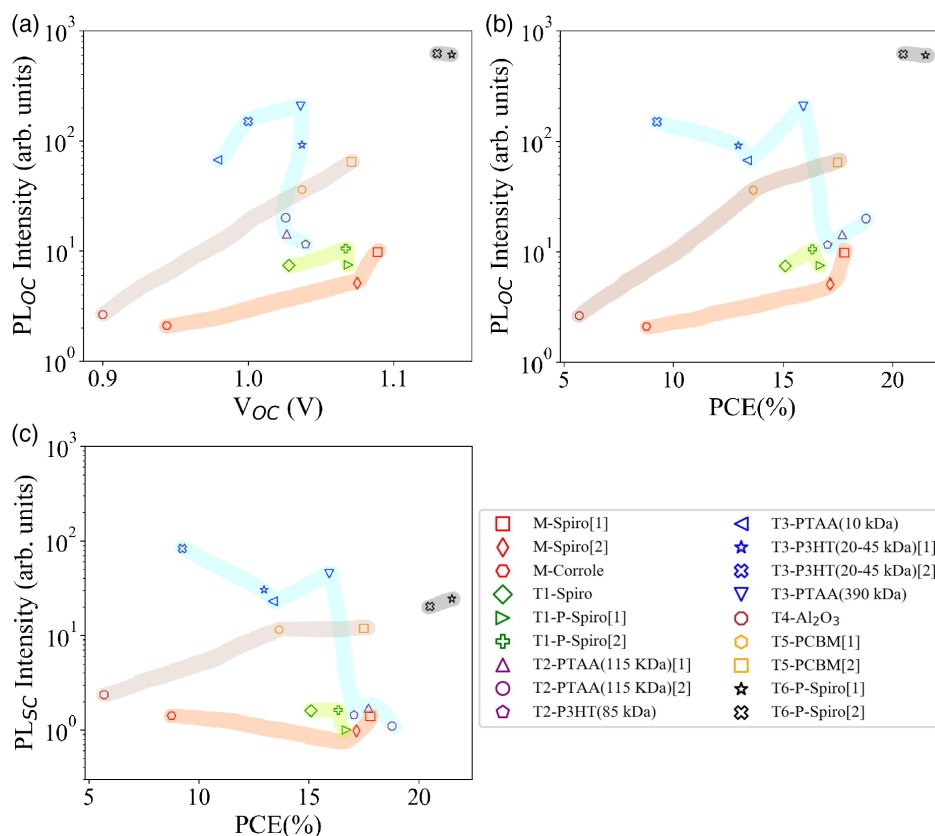


Figure 3. a) Logarithmic plot of the integrated PL intensity in OC conditions versus V_{oc} . b) Logarithmic plot of the integrated PL intensity in OC conditions versus PCE. c) Logarithmic plot of the integrated PL intensity in SC conditions versus PCE. Individual marker colors represent a particular production run, while the highlighting colors nominally equal active material.

is the ideal current given by the extraction of all the excited carriers.

Finally, we wish to point out that even for the largest quenching values, a clearly measurable amount of PL remains under SC conditions: this suggests that the extraction time (τ_e) for charge carriers is not much shorter than their lifetime. Considering that the PLQ curve (Figure 2) is mostly determined by the ratio between the two rates (k_1^{oc} and k_e), we estimate such ratio from the model: to obtain the observed PLQ_{oc-sc} (ranging between $\approx 15\%$ and $\approx 95\%$) we must have a τ_1/τ_e ratio of approximately 0.26 to 4 (see Figure S1c in Supporting Information). We bring to the reader's attention that with this simplified model, once one has a reference for τ_1 , it is possible to estimate τ_e of a device only using cw-PL measurements.

Clearly, we cannot ensure that PLQ_{oc-sc} is a foolproof and precise FOM in any circumstances as it is subject to different approximations. Nevertheless, it gives surprisingly good and general results, which appear more reliable than those obtained with simpler approaches, especially considering that the use of PLQ_{oc-sc} is also a fast method that can be applied with standard PL equipment and that gives further information of carrier dynamics.

We have mentioned above that the temporal instability of the PL intensity affects the choice of the correct values to evaluate PLQ_{oc-sc}. This instability of the PL intensity under illumination

has been carefully characterized and the analysis is presented in the SI (and summarized in Figure 1) along with the detailed description of how we have chosen the PL intensity values to be used in Equation (5). In general, under OC conditions, strong and nonmonotonous variations occur over all the observed time range (Figure S4, Supporting Information). These variations, already well known in halide perovskites, may be due to the creation and the annihilation of defects, introduced by light-activated mobile ions.^[29–38]

Another important aspect of the PSCs is that in SC conditions, not only the PL intensity varies in time but also I_{sc} . Indeed, as soon as the devices are switched to SC, in Figure S4, Supporting Information we observe a sudden quenching of the PL from its value at OC but as time passes the PL integrated intensity increases for all the devices, while an opposite trend is observed for the values of the I_{sc} , as shown in Figure 4, where we report the PL intensity and the value of I_{sc} as a function of time for two representative devices. A more complete set of results are reported in Figure S6, Supporting Information. The opposite behavior of the two quantities is clear and quite easily understood in terms of the competition between carrier radiative recombination and extraction.

The contemporary decrease of I_{sc} and increase of PL cannot be attributed only to defect creation or annihilation because neither of them can justify both trends together. It is instead clear that,

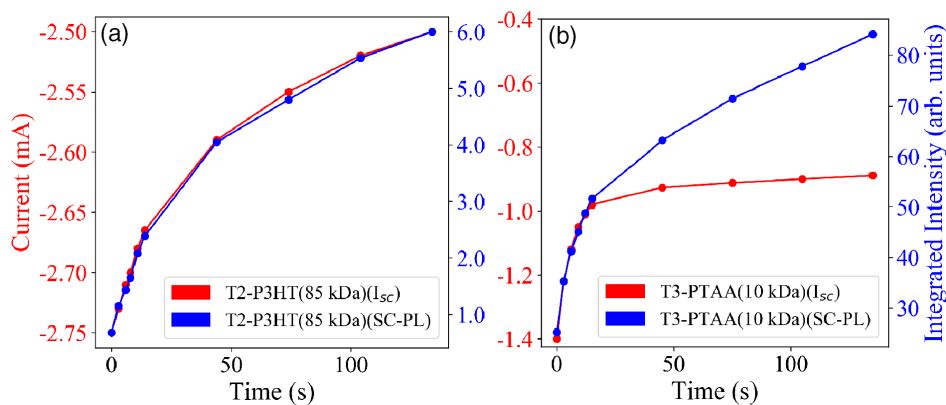


Figure 4. Variation of I_{sc} (red) and of the integrated PL intensity (blue) during the SC stage of measurement for two devices. The current decreases as the PL intensity increases.

over time, less carriers are able to leave the device and more carriers eventually recombine inside it, increasing the PL intensity. The reason why, as time goes by, fewer and fewer carriers are extracted from the device, can be found in an accumulation of ions at the interfaces between the perovskite and the extraction layers that build up a potential of opposite sign to that permitting carrier extraction.^[38] Our results also suggest that the defects, including those generated at the interfaces of the solar cells, are very important for PL_{oc} , but less so for PL_{sc} as demonstrated by the strong correlation between the current decrease and the PL increase. Indeed, there is no way to explain, with the presence or the creation of defects, the contemporary increase of the PL intensity, and the decrease of I_{sc} . If the two opposite trends are very similar in the first seconds, they can quantitatively differ at longer operation times. This difference observed from device to device needs further investigation to be understood.

While being aware that more statistics on a larger group of devices are necessary to confirm the general validity of this method and exclude any exceptions, we wish to point out that it is valid for any type of solar cell, independently of the active material used. Moreover, it is also very quick (the measurement can be performed in a few seconds) and does not require expensive instruments (once you know some characteristics of the active material, the measurement can be performed with a photodiode, a LED and an electrical switch). This would allow a quick and cheap efficiency evaluation on a large number of devices. With a deeper comprehension of the physics beneath the time variations of PL and its consequences on device performances, the same setup can also be used for monitoring the degradation of the devices.

4. Conclusions

In this work we have shown how the PL intensity should be used to characterize a photovoltaic cell based on perovskites. We confirm that considering the values of the PL intensity both at OC and SC it is possible to correlate the PL intensity to the device PCE through a single FOM based on the quenching of the PL observed in SC conditions (PLQ_{oc-sc}). We give an explanation of the observed correlation between PLQ_{oc-sc} and the PCE of

the device by means of a simplified model based on the carrier density rate equation. We have also shown that the analysis of PLQ_{oc-sc} using our model can provide a tool to estimate the carrier extraction time in PSCs through a simple cw-PL measurement, provided the carrier lifetime in OC conditions. Without suggesting that a PL measurement can substitute a $J-V$ characterization, we point out that this kind of measurement is very easy and the necessary instrumentation unexpensive and compact, so it could be implemented in a large-scale production or in small research laboratories that work at the early stages of solar cell development. Moreover, a clear correlation between the increase over time of the PL intensity in SC conditions and the contemporary decrease of the device current, I_{sc} , has been found.

Supporting Information

Supporting Information is available from the Wiley Online Library or from the author.

Acknowledgements

The authors gratefully acknowledge the financial support of Regione through ISIS@MACH (IR approved by Giunta Regionale n. G10795, August 7, 2019, published by BURL n. 69, August 27, 2019). A.A. and S.P. gratefully acknowledge the funding from the European Union's Horizon 2020 research and innovation program under grant agreement no. SGA 881603 GrapheneCore3. N.Y.N. acknowledges the support of the Italian Ministry of Economic Development in the framework of the Operating Agreement with ENEA for Research on the Electric System. B.Y. acknowledges funding from the European Union's Horizon 2020 research and innovation program under grant agreement no. 764047. J.S. acknowledges the support from Swiss National Science Foundation for financial support with project no. 200020_185041. F.D.G. thanks the ESPReso project (Horizon 2020, grant no. 764047) for funding.

Open Access Funding provided by Consiglio Nazionale delle Ricerche within the CRUI-CARE Agreement.

Conflict of Interest

The authors declare no conflict of interest.

Author Contributions

V.C., F.M., and A.D.C. conceived this project. V.C. performed the measurements and the analysis of the results with the help and supervision of F.M. The results were discussed among all the authors. The devices were fabricated and the related J - V measurements were performed by A.A. (M and T1), S.P. (M and T1), N.Y.N. (T2 and T3), and F.D.G. (T4 and T5), and all of them also wrote the related experimental section. F.D.G. performed the J - V measurements for the T6 devices, which were fabricated by B.Y. and J.S. A.A., S.P., and N.Y.N. contributed to design the optimal device configuration for PL measurements. V.C. and F.M. wrote the first draft of the manuscript and all authors contributed to its final form.

Data Availability Statement

The data that support the findings of this study are available from the corresponding author upon reasonable request.

Keywords

perovskites, photoluminescence, solar cells

Received: February 2, 2022

Revised: April 28, 2022

Published online: May 14, 2022

- [1] D. W. deQuilettes, K. Frohna, D. Emin, T. Kirchartz, V. Bulovic, D. S. Ginger, S. D. Stranks, *Chem. Rev.* **2019**, *119*, 11007.
- [2] T. Kirchartz, J. A. Márquez, M. Stolterfoht, T. Unold, *Adv. Energy Mater.* **2020**, *10*, 1904134.
- [3] J. Richter, M. Abdi-Jalebi, A. Sadhanala, M. Tabachnyk, J. P. H. Rivett, L. M. Pazos-Outón, K. C. Gödel, M. Price, F. Deschler, R. H. Friend, *Nat. Commun.* **2016**, *7*, 13941.
- [4] P. Caprioglio, M. Stolterfoht, C. M. Wolff, T. Unold, B. Rech, S. Albrecht, D. Neher, *Adv. Energy Mater.* **2019**, *9*, 1901631.
- [5] S. Kavadiya, A. Onno, Caleb C. Boyd, X. Wang, A. Cetta, M. D. McGehee, Z. C. Holman, *Sol. RRL*, **2021**, *5*, 2100107.
- [6] E. Yablonovitch, O. D. Miller, S. R. Kurtz, *AIP Conf. Proc.* **2013**, *1519*, 9.
- [7] R. T. Ross, *J. Chem. Phys.* **1967**, *46*, 4590.
- [8] U. Rau, *Phys. Rev. B* **2007**, *76*, 085303.
- [9] M. Stolterfoht, P. Caprioglio, C. M. Wolff, J. A. Márquez, J. Nordmann, S. Zhang, D. Rothhardt, U. Hörmann, Y. Amir, A. Redinger, L. Kegelmann, F. Zu, S. Albrecht, N. Koch, T. Kirchartz, M. Saliba, T. Unold, D. Neher, *Energy Environ. Sci.* **2019**, *12*, 2778.
- [10] M. Auf der Maur, A. Di Carlo, *Sol. Energy*, **2019**, *187*, 358.
- [11] H. Coskun, F. H. Isikgor, Z. Chen, M. Imran, B. Li, Q. Xu, J. Ouyang, *J. Mater. Chem. A* **2019**, *7*, 4759.
- [12] X. Jin, X. Lei, C. Wu, G. Jiang, W. Liu, H. Zeng, T. Chen, C. Zhu, *J. Mater. Chem. A* **2017**, *5*, 19884.
- [13] J. Wang, J. Xu, Z. Li, X. Lin, C. Yu, H. Wu, H. Wang, *ACS Applied Energy Materials* **2020**, *3*, 6344.
- [14] F. Wang, M. Endo, S. Mouri, Y. Miyauchi, Y. Ohno, A. Wakamiya, Y. Murata, K. Matsuda, *Nanoscale* **2016**, *8*, 11882.
- [15] C. Xu, Z. Liu, E.-C. Lee, *J. Mater. Chem. C* **2018**, *6*, 6975.
- [16] X.-H. Zhang, J.-J. Ye, L.-Z. Zhu, H.-Y. Zheng, X.-P. Liu, X. Pan, S.-Y. Dai, *ACS Appl. Mater. Interfaces* **2016**, *8*, 35440.
- [17] L. Xu, L.-L. Deng, J. Cao, X. Wang, W.-Y. Chen, Z. Jiang, *Res. Lett.* **2017**, *12*, 159.
- [18] M. Stolterfoht, C. M. Wolff, J. A. Márquez, S. Zhang, C. J. Hages, D. Rothhardt, S. Albrecht, P. L. Burn, P. Meredith, T. Unold, D. Neher, *Nat. Energy* **2018**, *3*, 847.
- [19] M. Stolterfoht, V. M. Le Corre, M. Feuerstein, P. Caprioglio, L. J. A. Koster, D. Neher, *ACS Energy Lett.* **2019**, *4*, 2887.
- [20] C. Dreesen, D. P. del-Rey, P. P. Boix, H. J. Bolink, *J. Lumin.* **2020**, *222*, 117106.
- [21] T. Du, W. Xu, M. Daboczi, J. Kim, S. Xu, C.-T. Lin, H.; Kang, K.; Lee, M. J. Heeney, J.-S. Kim, J. R. Durrant, M. A. McLachlan, *J. Mater. Chem. A* **2019**, *7*, 18971.
- [22] K. Tvingstedt, O. Malinkiewicz, A. Baumann, C. Deibel, H. J. Snaith, V. Dyakonov, H. J. Bolink, *Sci. Rep.* **2014**, *4*, 6071.
- [23] K. Tvingstedt, K. Vandewal, F. Zhang, O. Inganäs, *J. Phys. Chem. C* **2010**, *114*, 21824.
- [24] U. Rau, V. Huhn, B. E. Pieters, *Phys. Rev. Applied* **2020**, *14*, 014046.
- [25] D. Hinken, K. Bothe, K. Ramspeck, S. Herlufsen, R. Brendel, *J. of Appl. Phys.* **2009**, *105*, 104516.
- [26] C.-T. Lin, W. Xu, T. J. Macdonald, J. Ngiam, J.-H. Kim, T. Du, S. Xu, P. S. Tuladhar, H. Kang, K. Lee, J. R. Durrant, and M. A. McLachlan, *ACS Appl. Mater. Interfaces* **2021**, *13*, 43505.
- [27] E. Regalado-Pérez, Evelyn B. Díaz-Cruz, J. Landa-Bautista, N. R. Mathews, X. Mathew, *ACS Appl. Mater. Interfaces* **2021**, *13*, 11833.
- [28] T. Du, W. Xu, S. Xu, S. R. Ratnasingham, C.-T. Lin, J. Kim, J. Briscoe, M. A. McLachlan, J. R. Durrant, *J. Mater. Chem. C* **2020**, *8*, 12648.
- [29] Y. Tian, M. Peter, E. Unger, M. Abdellah, K. Zheng, T. Pullerits, A. Yartsev, V. Sundströma, I. G. Scheblykin, *Phys. Chem. Chem. Phys.* **2015**, *17*, 24978.
- [30] J. F. Galisteo-López, M. Anaya, M. E. Calvo, H. Míguez, *J. of Phys. Chem. Lett.* **2015**, *6*, 2200.
- [31] X. Fu, D. A. Jacobs, F. J. Beck, T. Duong, H. Shen, K. R. Catchpole, T. P. White, *Phys. Chem. Chem. Phys.* **2016**, *18*, 22557.
- [32] D. deQuilettes, W. Zhang, V. Burlakov, D. J. Graham, T. Leijtens, A. Osherov, V. Bulović, H. J. Snaith, D. S. Ginger, S. D. Stranks, *Nat Commun.* **2016**, *7*, 11683.
- [33] H. Lou, C. Lin, Z. Fang, L. Jiang, X. Chen, Z. Ye, H. He, *RSC Adv.* **2020**, *10*, 11054.
- [34] X. Wen, S. Huang, S. Chen, X. Deng, F. Huang, Cheng, Yi-Bing, M. Green, A. Ho-Baillie, *Adv. Mater. Interfaces* **2016**, *3*, 1600467.
- [35] Y. Zhong, C. A. Melo Luna, R. Hildner, C. Li, S. Huettner, *APL Materials* **2019**, *7*, 041114.
- [36] W. Nie, J. C. Blancon, A. Neukirch, K. Appavoo, H. Tsai, M. Chhowalla, M. A. Alam, M. Y. Sfeir, C. Katan, J. Even, S. Tretiak, J. J. Crochet, G. Gupta, A. D. Mohite, *Nat Commun* **2016**, *7*, 11574.
- [37] R. Gottesmanan, L. Gouda, B. S. Kalanoor, E. Haltzi, S. Tirosh, E. Rosh-Hodesh, Y. Tischler, A. Zaban, C. Quarti, E. Mosconi, F. De Angelis, *J. Phys. Chem. Lett.* **2015**, *6*, 2332.
- [38] X. Deng, X. Wen, J. Zheng, T. Young, C. F. J. Lau, J. Kim, M. Green, S. Huang, A. Ho-Baillie, *Nano Energy* **2018**, *46*, 356.
- [39] A. Agresti, B. Berionni, S. Pescetelli, A. Catini, F. Menchini, C. Di, R. Paolesse, A. Di Carlo, *Adv. Funct. Mater.* **2020**, *30*, 2003790.
- [40] T. Zhu, D. Zheng, J. Liu, L. Coolen, Thierry Pauporté, *ACS Appl. Mater. Interfaces* **2020**, *12*, 37197.
- [41] N. Y. Nia, M. Zendeherdel, M. Abdi-Jalebi, L. A. Castriotta, F. U. Kosasih, E. Lamanna, M. M. Abolhasani, Z. Zheng, Z. Andaji-Garmaroudi, K. Asadi, G. Divitini, C. Ducati, R. H. Friend, A. Di Carlo, *Nano Energy* **2021**, *82*, 105685.
- [42] N. Yaghoobi Nia, M. Méndez, A. Di Carlo, E. Palomares, *Philos. Trans. A Math. Phys. Eng. Sci.* **2019**, *377*, 20180315.
- [43] F. Di Giacomo, L. A. Castriotta, F. U. Kosasih, D. Di Girolamo, C. Ducati, A. Di Carlo, *Micromachines* **2020**, *11*, 1127.

- [44] A. Agresti, A. Pazniak, S. Pescetelli, A. Di Vito, D. Rossi, A. Pecchia, M. Auf der Maur, A. Lied, R. Larciprete, D. V. Kuznetsov, D. Saranin, A. Di Carlo, *Nat. Mater.* **2019**, *18*, 1228-.
- [45] M. Saliba, T. Matsui, J.-Y. Seo, K. Domanski, J.-P. Correa-Baena, M. K. Nazeeruddin, S. M. Zakeeruddin, W. Tress, A. Abate, *Energy Environ. Sci.* **2016**, *9*, 1989.
- [46] L. Krückemeier, U. Rau, M. Stolterfoht, T. Kirchartz, *Adv. Energy Mater.* **2020**, *10*, 1902573.
- [47] M. Saidaminov, A. M. Abdelhady, B. Murali, E. Alarousu, V. M. Burlakov, W. Peng, I. Dursun, L. Wang, Y. He, G. Maculan, A. Goriely, T. Wu, O. F. Mohammed, O. M. Bakr, *Nat Commun* **2015**, *6*, 7586.
- [48] A. M. A. Leguy, P. A. Azarhoosh, M. I. Alonso, M. Campoy-Quiles, O. J. M. Weber, O. J. Yao, *Nanoscale* **2015**, *8*, 6317.
- [49] V. Campanari, A. Agresti, S. Pescetelli, A. K. Sivan, D. Catone, P. O’Keeffe, S. Turchini, A. Di Carlo, F. Martelli, *Phys. Rev. Mater.* **2021**, *5*, 035409.
- [50] W.-A. Quitsch, D. W. deQuilettes, O. Pflingsten, A. Schmitz, S. Ognjanovic, S. Jariwala, S. Koch, M. Winterer, *J. Phys. Chem. Lett.* **2018**, *9*, 2062.
- [51] M. B. Johnston, L. M. Herz, *Acc. Chem. Res.* **2016**, *49*, 146.
- [52] A. Al-Ashouri, A. Magomedov, M. Roß, M. Jošt, M. Talaikis, G. Chistiakova, T. Bertram, J. A. Márquez, E. Köhnen, E. Kasparavičius, S. Levenco, L. Gil-Escrig, C. J. Hages, R. Schlatmann, B. Rech, T. Malinauskas, T. Unold, C. A. Kaufmann, L. Korte, G. Niaura, V. Getautis, S. Albrecht, *Energy Environ. Sci.*, **2019**, *12*, 3356.
- [53] M. Bonn, K. Miyata, E. Hendry, X.-Y. Zhu, *ACS Energy Lett.* **2017**, *2*, 2555.
- [54] F. Zheng, L. Z. Tan, S. Liu, A. M. Rappe, *Nano Lett.* **2015**, *15*, 7794.
- [55] L. M. Pazos-Outón, M. Szumilo, R. Lamboll, J. M. Richter, M. Crespo-Quesada, M. Abdi-Jalebi, H. J. Beeson, M. Vručinić, M. Alsari, H. J. Snaith, B. Ehrler, R. H. Friend, Felix Deschler, *Science* **2016**, *351*, 1430.